JOURNAL OF PROPULSION AND POWER
Vol. 22, No. 1, January–February 2006

Effect of Tip Clearance on the Cavitation Performance of a Turbopump Inducer

Soon-Sam Hong,* Jin-Sun Kim,† Chang-Ho Choi,* and Jinhan Kim‡
Korea Aerospace Research Institute, Daejeon 305-333, Republic of Korea

The characteristics of steady and unsteady cavitation in a two-bladed inducer for a turbopump are investigated. A helical inducer with inlet tip blade angle of 7.8 deg and a tip solidity of 2.7 is tested using water as a working fluid. To determine the effect of tip clearance on the inducer performance, a series of experiments is conducted at three different tip clearances. As the tip clearance increases, the inducer head decreases and the critical cavitation number increases. Unsteady pressure measurements at the inducer inlet indicate the existence of attached cavitation and cavitation surge, but no rotating cavitation in the test inducer. Attached cavitation and cavitation surge appear for all three cases of tip clearance. The cell number and propagation speed of the attached cavitation are determined through a cross-correlation analysis. In the case of attached cavitation, one cell rotates at the same speed as that of the inducer. In addition, the surge frequency decreases with a decrease in the cavitation number, and the ratio of surge frequency to inducer rotational frequency is found to range from 0.07 to 0.20.

Nomenclature

c	=	tip clearance
f_{CS}	=	oscillating frequency of cavitation surge
f_N	=	inducer rotational frequency
H	=	inlet blade height
h	=	inducer total head
p_v	=	vapor pressure
p_{01}	=	inlet total pressure
p'	=	pressure fluctuation
Q	=	flow rate
Q_n	=	nominal flow rate
U_{1t}	=	inducer tip speed
$\Delta\psi$	=	coefficient of inlet pressure fluctuation, $p'/(0.5\rho U_{1t}^2)$
σ	=	cavitation number, $(p_{01} - p_v)/(0.5\rho U_{1t}^2)$
σ_{cr}	=	critical cavitation number
ψ	=	head coefficient, $h/(U_{1t}^2/2g)$

Introduction

WITHIN a liquid rocket engine turbopump, inducers are often placed upstream of the main impeller to improve the cavitation performance. They pressurize the flow sufficiently to enable the main centrifugal impeller to operate without cavitation. However, inducers often suffer from cavitation instabilities such as rotating cavitation, cavitation surge, and attached cavitation.

Many studies[1–6] on inducer cavitation have been conducted, but most of them are experimental due to the difficulties in prediction by numerical modeling. Hashimoto et al.[1] observed supersynchronous shaft vibrations in the inducer of a liquid oxygen turbopump for the LE-7 engine. They concluded that these shaft vibrations were caused by rotating cavitation. A simple modification to the inducer housing almost completely eliminated the shaft vibrations. Tsujimoto et al.[2] investigated various forms of oscillating cavitation, such as rotating cavitation, attached cavitation, and surge mode oscillations. They found that the speed of the rotating cavitation was 1.1–1.3 times higher than that of the inducer with three blades. It is known that rotating cavitation occurs in the case of an odd number of blades and that attached cavitation appears in the case of an even number of blades. Uchiumi et al.[5] observed a noticeable deterioration of suction performance of the LE-7A fuel turbopump, and they found that the deterioration was a result of rotor vibration caused by a rotating-stall-type oscillation.

The blade tip clearance of an inducer should be as small as possible to reduce tip clearance losses, but always sufficient to preclude detrimental rubbing between the inducer and housing. The rubbing may induce explosions in the case of oxidizer pumps. A practically attained minimum value of the ratio of inducer tip clearance to blade height is 2% for oxidizer applications.[6] Janigro and Ferrini[7] investigated the effect of tip clearance on the cavitation performance of an inducer, but they did not consider cavitation-induced flow instabilities.

We have tested a number of turbopump inducers with various solidities[8] and blade angles[9] to determine the effect of these design parameters on steady-state performance. In this paper, cavitation instabilities and the effect of blade tip clearance on the inducer performance are presented.

Experimental Apparatus

The working fluid used for the test is water at room temperature. Figure 1 shows an outline of the test loop, where the main pipe line has a nominal diameter of 100 mm. The inducer is driven by a variable-speed motor with a capacity of 10,000 rpm and 37 kW. The flow rate is controlled by a regulating valve. The pressure of the water tank with 0.9-m^3 volume is adjusted by using a vacuum pump and compressed air. A booster pump is employed when the inducer head is not high enough to circulate water in the test loop. The booster pump has no effect on the inducer performance.

The inducer for the test (Fig. 2) is a scale model, two times larger than the original oxidizer pump inducer. Table 1 shows the geometry and operating condition of the inducer. The inlet flow coefficient is defined as the ratio of the mean axial velocity to the tip speed at the inducer inlet. Three cases of the tip clearance, defined as the radial gap between the inducer tip and the casing, were tested by using three casings with different inner diameters for the same test inducer. The clearance ratio c/H is defined as the ratio of the clearance c to the inlet blade height H (Fig. 3). The baseline clearance is 1.0 mm, which corresponds to the clearance ratio $c/H = 0.026$. For the present study, the rotational speed of the inducer is fixed at 6000 rpm with variation of 0.1%. The mean flow rate is measured by a turbine-type flow meter with the error less than 1%. The inducer head is evaluated from the pressure difference between the inlet settling chamber and the collector outlet. Four fast-response

Received 31 July 2004; revision received 25 April 2005; accepted for publication 2 May 2005.

*Senior Researcher, Turbopump Department. Member AIAA.
†Researcher, Turbopump Department.
‡Head of Department, Turbopump Department.

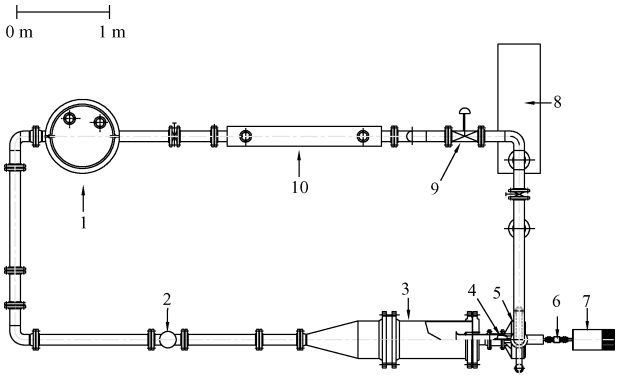

Fig. 1 Plane view of test loop: 1) water tank, 2) turbine flow meter, 3) settling chamber, 4) test inducer, 5) collector, 6) torque meter, 7) motor, 8) booster pump, 9) regulating value, and 10) heat exchanger.

Fig. 2 Test inducer.

pressure transducers (Kulite ETM-375 model with natural frequency of 285 kHz given by manufacturer) are installed 33-mm upstream of the inducer, at four evenly spaced circumferential locations, 90 deg apart as shown in Fig. 3. At each cavitation number, the four pressure signals are simultaneously acquired for 3 s at a 5-kHz sampling rate.

Results and Discussion

The comparison of noncavitating head performance of the inducer at the three levels of tip clearance is shown in Fig. 4, in which the head coefficient is plotted against the flow rate ratio. The head coefficient decreases linearly with the flow rate. At a nominal flow rate, the head coefficient decreases with the tip clearance. A study indicates that the loss in performance may be estimated from the

Table 1 Inducer geometry and operating condition

	Tip clearance c, mm		
Item	1.0	2.0	3.0
Clearance ratio, c/H	0.026	0.053	0.079
Inlet flow coefficient at nominal flow rate	0.073	0.070	0.067
Inlet blade height H, mm		38	
Inlet tip diameter, mm		106	
Outlet tip diameter, mm		78	
Inlet tip blade angle, deg		7.8	
Outlet tip blade angle, deg		13.2	
Sweepback angle of leading edge, deg		20	
Inlet tip blade thickness, mm		1.5	
Blade number		2	
Tip solidity		2.7	
Axial length of blade on the hub, mm		88	
Rotational speed, rpm		6,000	
Nominal flow rate Q_n at 6000 rpm, l/s		20.5	

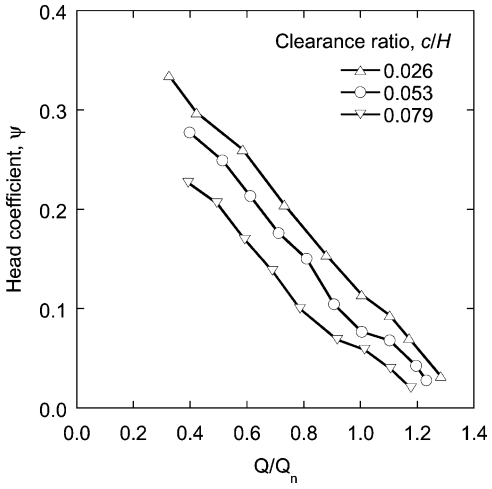

Fig. 4 Head characteristics of inducer.

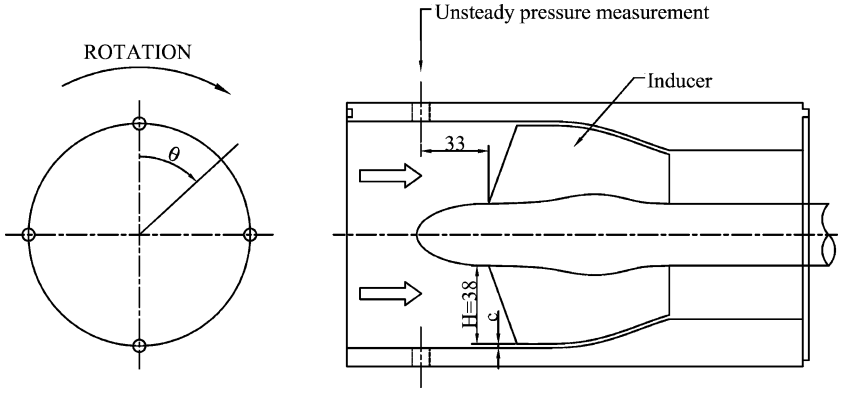

Fig. 3 Inducer test section and unsteady pressure measurement location.

following empirical relationship[6]:

$$\psi = \psi_0\left(1 - k\sqrt{c/H}\right) \tag{1}$$

We obtained $\psi_0 = 0.188$ and $k = 2.47$ from the curve fitting of the current test result, as shown in Fig. 5.

The cavitation characteristics of the inducer are presented in Fig. 6 at three different tip clearances. The data for $c/H = 0.079$ at $Q/Q_n = 1.2$ were not available due to the system head loss of the test loop. In Fig. 6, points for the unsteady cavitation such as attached cavitation and cavitation surge are marked. To investigate these unsteady cavitation phenomena, a spectral analysis of the inlet pressure fluctuation at $c/H = 0.026$ and $Q = Q_n$ was conducted (Fig. 7).

In Fig. 7, results of the spectral analysis are displayed at the region of cavitation number $\sigma < 0.2$ of Fig. 6a. When the cavitation number σ is decreased, attached cavitation is first observed at $\sigma = 0.107$. Note that peaks at rotational frequency f_N are also found at region of $\sigma > 0.107$ in Fig. 7, but the peaks increase significantly during attached cavitation. The cell number and frequency of the attached

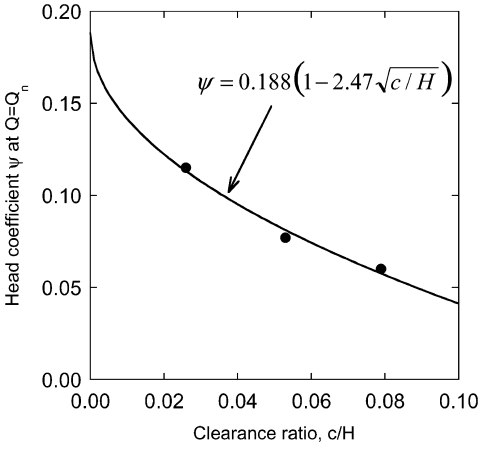

Fig. 5 Head vs tip clearance at nominal flow rate.

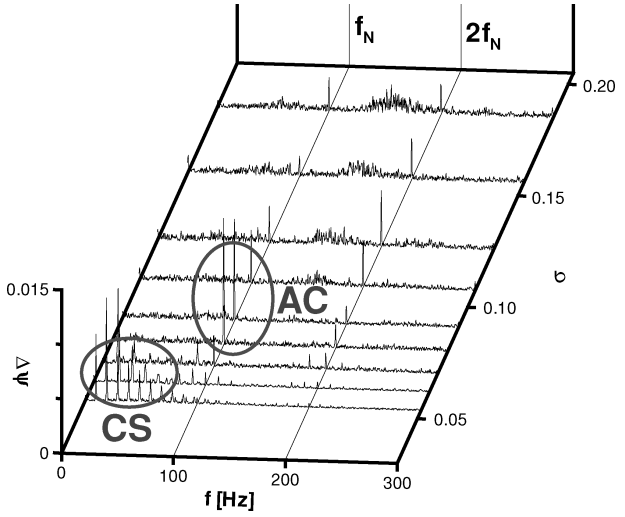

Fig. 7 Spectral analysis of inlet pressure fluctuation for $c/H = 0.026$ at $Q = Q_n$: attached cavitation (AC) and cavitation surge (CS).

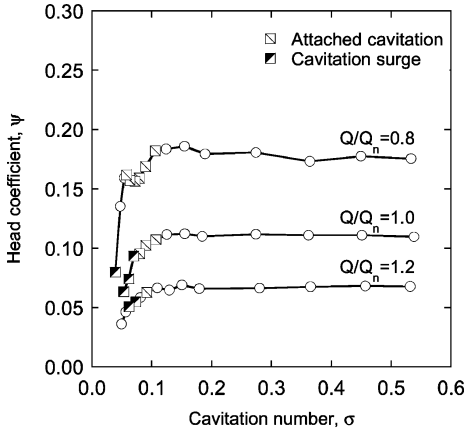

a) $c/H = 0.026$

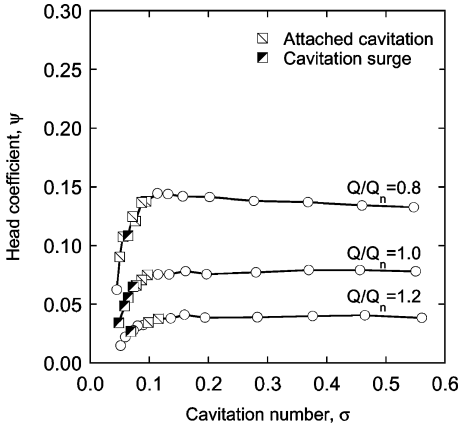

b) $c/H = 0.053$

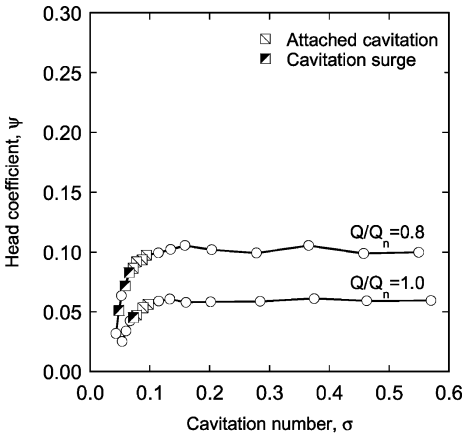

c) $c/H = 0.079$

Fig. 6 Cavitation performance curve of inducer.

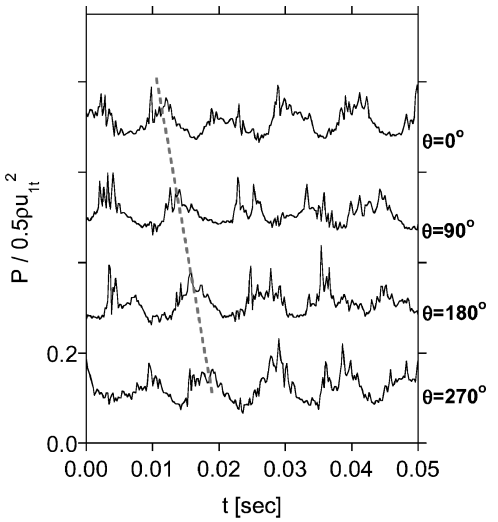

a) Pressure signal at four circumferential locations

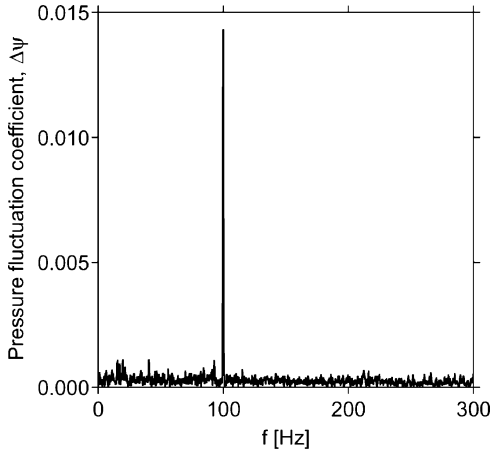

b) Spectrum of inlet pressure fluctuation at $\theta = 0$ deg

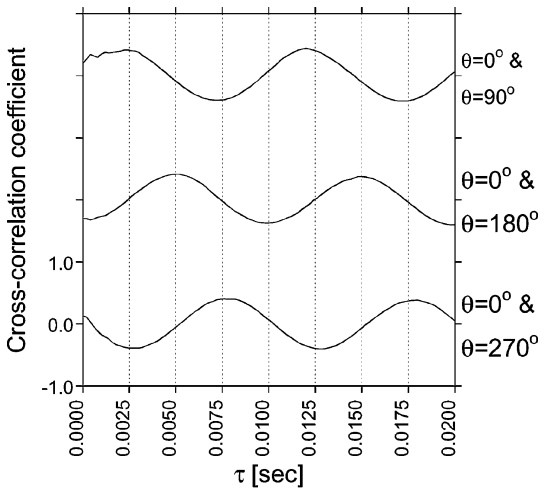

c) Cross-correlation coefficients

Fig. 8 Inlet pressure at attached cavitation for $c/H = 0.026$ at $\sigma = 0.08$, $Q = Q_n$.

cavitation will be identified later. With a further decrease in the cavitation number, cavitation surge is observed at $\sigma \leq 0.07$. Violent oscillations in the pressure and the flow rate in the entire system occur when cavitation surge is initated.

The cross-correlation coefficients of the unsteady pressure signals obtained from four unsteady pressure transducers installed at the inducer inlet are analyzed to investigate whether the cavitation cells rotate. Figure 8 shows an example of the analysis with $c/H = 0.026$ at $\sigma = 0.08$ and $Q = Q_n$. Time signals of unsteady pressure measured at four evenly spaced circumferential locations are shown in Fig. 8a, in which the ordinate is the coefficient of absolute pressure normalized by $0.5\rho U_{1t}^2$. A time lag is observed at two adjacent signals, which implies that the pressure pattern rotates circumferentially. The Fourier transform of the pressure signal at $\theta = 0$ deg is shown in Fig. 8b, where 100 Hz is the dominant frequency. The cross-correlation coefficients of pressure signals at $\theta = 90$, 180, and 270 deg, compared to the signal at $\theta = 0$ deg, are shown in Fig. 8c.

The cell number and propagation speed of the attached cavitation are determined from the following formula[10]:

$$m = (2\pi/\Delta\theta)(\tau_1/\tau_2) \tag{2}$$

$$f_s = 2\pi/m\tau_2 \tag{3}$$

where m is the number of cells, $\Delta\theta$ is the angular displacement between two sensors, τ_1 is a time lag between two signals, τ_2 is a period of periodic signals at two sensors, and f_s is an angular propagation speed of the cells. When this method is applied to the pressure signals in Fig. 8, it is found that one cell rotates at 100 Hz, which is the same frequency as the inducer rotational frequency, 6000 rpm (100 Hz). This implies that one cell fixed to the rotating inducer rotates at the speed same as the inducer. This might correspond to attached uneven cavitation for the case with an odd number (three) of blades.[2] Tsujimoto et al.[2] observed one shorter cavity and two longer cavities fixed to three blades of the rotating inducer by using a high-speed camera. They found that one cell rotated at the same speed as the inducer from the spectral analysis of the inlet pressure fluctuations.

Figure 9 shows the Fourier transforms of the signals at each flow rate at three different tip clearances. At $c/H = 0.026$, the amplitude of the pressure fluctuation of the attached cavitation increases but that of the cavitation surge decreases when Q/Q_n decreases from 1.0 to 0.8. The amplitude of the pressure fluctuation at $Q/Q_n = 1.2$ is lower than that at $Q/Q_n = 0.8$ and 1.0. The pattern of the pressure fluctuation amplitude at $c/H = 0.053$ is similar to that at $c/H = 0.026$. At $c/H = 0.079$, the pressure fluctuation amplitude decreases noticeably. It is found that one cell of the attached cavitation rotates at 100 Hz for the three clearance levels tested. Rotating cavitation is known to rotate faster than the inducer.[2] For the test inducer, rotating cavitation was not observed.

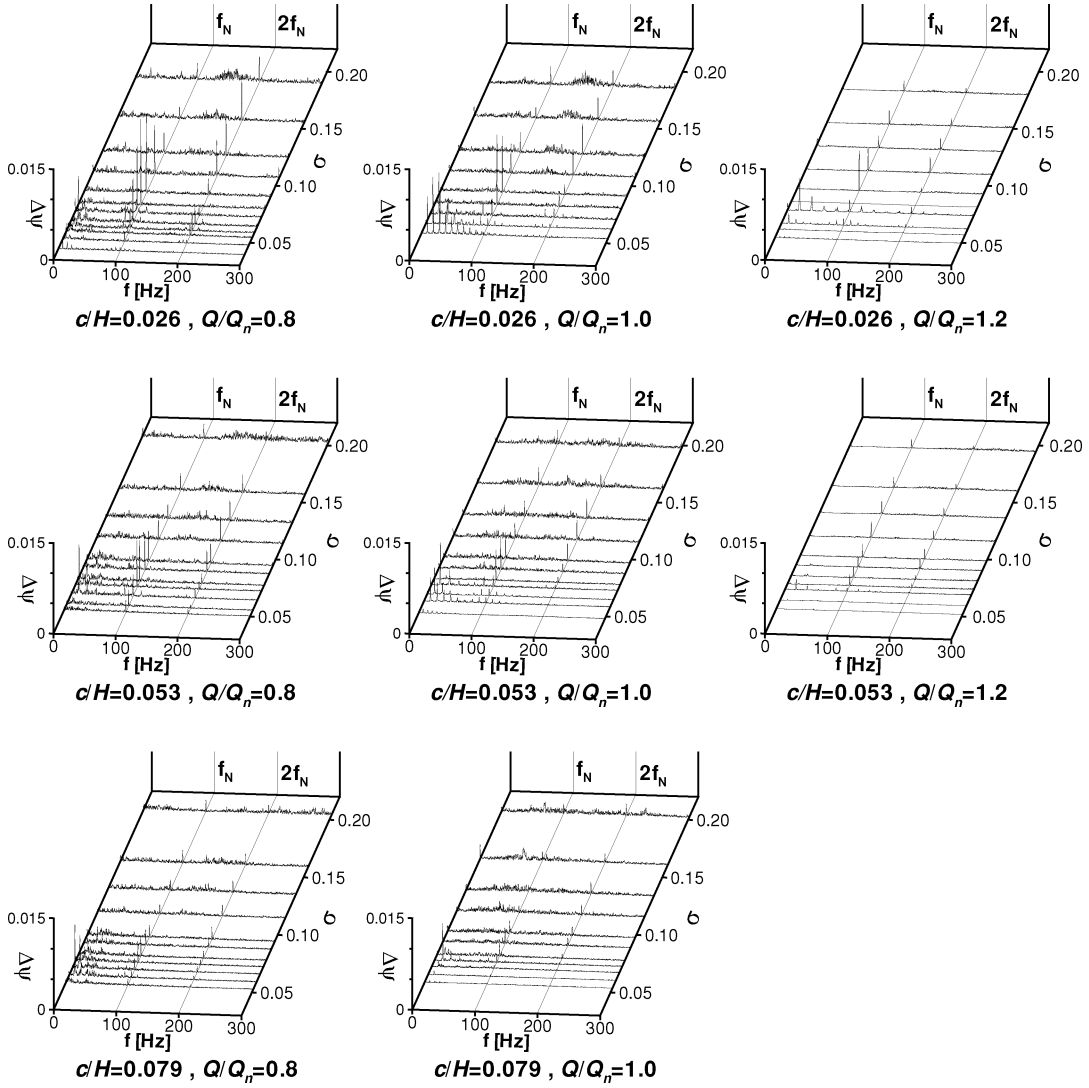

Fig. 9 Spectral analysis of inlet pressure fluctuations at three levels of tip clearance.

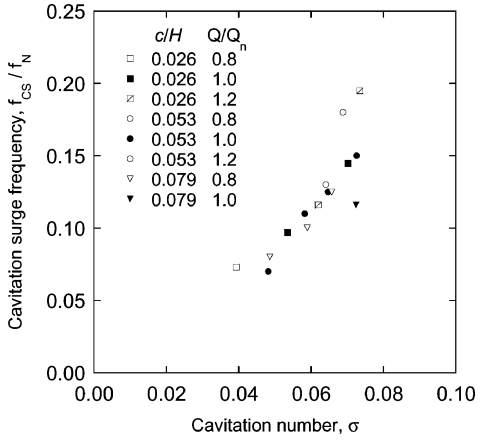

Fig. 10 Ratio of oscillating frequency of cavitation surge to inducer rotational frequency.

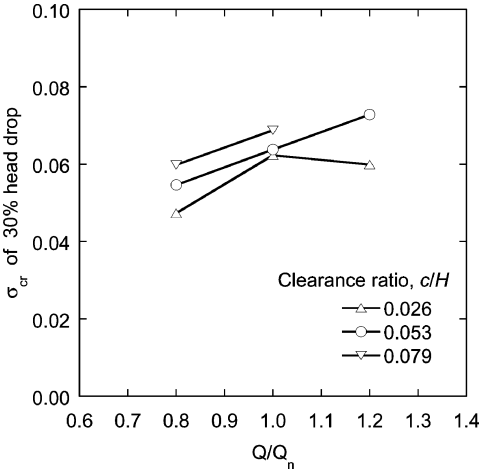

Fig. 11 Critical cavitation number vs flow rate.

Table 2 Oscillating frequency of cavitation surge

	c/H		
Q/Q_n	0.026	0.053	0.079
0.8	7 Hz	13 Hz	8–12 Hz
1.0	10–15 Hz	7–15 Hz	13 Hz
1.2	12–20 Hz	18 Hz	

The oscillating frequency of cavitation surge depends on the tip clearance and flow parameters. The oscillating frequency for each flow rate is summarized in Table 2. Figure 10 shows how the reduced surge frequency, f_{CS}/f_N, varies with flow rate, tip clearance, and cavitation number. Whereas the surge frequency shows no clear dependence on either the flow rate or the tip clearance, it decreases with decreasing cavitation number. The reduced surge frequency ranges from 0.07 to 0.20.

Figure 11 presents the critical cavitation numbers, which are derived from the cavitation performance curves of Fig. 6. The critical cavitation number σ_{cr} is defined as the cavitation number where the head drops by 30% of the head at a noncavitating condition. One usually looks for at least 10% head drop as σ_{cr}, and it is not uncommon to consider a 50% head drop.[11] The critical cavitation number increases with an increase in the flow rate. At the same flow rate, the critical cavitation number increases with an increase in tip clearance. The clearance effect on the critical cavitation number, however, is small at the nominal flow rate.

Conclusions

Three cases of tip clearance were tested for a two-bladed inducer. With increasing tip clearance, the inducer head decreased and the critical cavitation number increased. Attached cavitation and cavitation surge were observed at all levels of tip clearance. During attached cavitation, one cell rotated at the same speed as the inducer. The surge frequency decreased with decreasing cavitation number, and the ratio of surge frequency to inducer rotational frequency varied from 0.07 to 0.20.

References

[1]Hashimoto, T., Yoshida, M., Watanabe, M., Kamijo, K., and Tsujimoto, Y., "Experimental Study on Rotating Cavitation of Rocket Propellant Pump Inducers," *Journal of Propulsion and Power*, Vol. 13, No. 4, 1997, pp. 488–494.

[2]Tsujimoto, Y., Yoshida, Y., Maekawa, Y., Watanabe, S., and Hashimoto, T., "Observations of Oscillating Cavitation of an Inducer," *Journal of Fluids Engineering*, Vol. 119, No. 4, 1997, pp. 775–781.

[3]Yoshida, Y., Tsujimoto, Y., Kataoka, D., Horiguchi, H., and Wahl, F., "Effect of Alternate Leading Edge Cutback on Unsteady Cavitation in 4-Bladed Inducers," *Journal of Fluids Engineering*, Vol. 123, No. 4, 2001, pp. 762–770.

[4]Furukawa, A., Ishizaka, K., and Watanabe, S., "Experimental Study of Cavitation Induced Oscillation in Two Bladed Inducers," *Proceedings of the 4th International Conference on Launcher Technology, Space Launcher Liquid Propulsion*, Centre National d'Etudes Spatiales, Paris, Dec. 2002.

[5]Uchiumi, M., Kamijo, K., Hirata, K., Konno, A., Hashimoto, T., Kobayasi, S., "Improvement of Inlet Flow Characteristics of LE-7A Liquid Rocket Hydrogen Pump," *Journal of Propulsion and Power*, Vol. 19, No. 4, 2003, pp. 356–363.

[6]Jakobsen, J. K., *Liquid Rocket Engine Turbopump Inducers*, NASA SP-8052, May 1971, pp. 62, 63.

[7]Janigro, A., and Ferrini, F., "Inducer Pumps," *Recent Progress in Pump Research*, Lecture Series 61, von Karman Inst. for Fluid Dynamics, Rhode-Saint-Genese, Belgium, 1973.

[8]Hong, S., Choi, C., and Kim, J., "Effect of Solidity on the Performance of Turbopump Inducer," *Transactions of Korean Society of Mechanical Engineers, Ser. B*, Vol. 28, No. 4, 2002, pp. 382–388 (in Korean).

[9]Kim, J., Hong, S., Choi, C., Kim, J., and Cho, K., "Effect of Blade Angle on the Performance of Turbopump Inducer," *Proceedings of the Korean Society of Aeronautical and Space Sciences Fall Conference*, Korean Society of Aeronautical and Space Sciences, Seoul, Korea, Nov. 2003, pp. 1059–1062 (in Korean).

[10]Frigne, P., and Van Den Braembussche, R., "Distinction between Different Types of Impeller and Diffuser Rotating Stall in a Centrifugal Compressor with Vaneless Diffuser," *Journal of Engineering for Gas Turbines and Power*, Vol. 106, April 1984, pp. 468–474.

[11]Japikse, D., "Overview of Commercial Pump Inducer Design," *Proceedings of the 9th International Symposium on Transport Phenomena and Dynamics of Rotating Machinery*, Pacific Center of Thermal-Fluids Engineering, HI, Feb. 2002.